Limit states design calibration for geogrid pullout in reinforced soil walls

Bingquan Huang
GeoEngineering Centre at Queen's-RMC,
Department of Civil Engineering, Queen's University, Kingston, Ontario, Canada
Richard J. Bathurst
GeoEngineering Centre at Queen's-RMC,
Department of Civil Engineering, Royal Military College of Canada, Kingston, Ontario, Canada

ABSTRACT
Limit states design (LSD) calibration for reinforced soil retaining wall design has until recently been restricted to comparison to allowable stress design (ASD) practice (often called "calibration by fitting"). This paper is focused on LSD calibration for the case of reinforcement pullout in geogrid reinforced soil walls. A unique feature of the paper is a pullout resistance database of more than 300 data points that provides sufficient statistical data to carry out the calibration. The framework adopted in this study is based on the approach reported by Bathurst et al. (2008a). Five different deterministic pullout models, including the current default AASHTO/FHWA pullout model, and the default load factor of 1.35 recommended by AASHTO, are used in the calibration. The target probability of failure is taken as 1 in 100. To simplify the examples in the paper, load bias statistics are assumed. Deterministic models are investigated for hidden dependencies and a new pullout model is proposed. Calibration results are presented in the form of tables of resistance factors.

RÉSUMÉ
Le calibrage des méthodes de calcul aux états limites (LSD) pour le design des murs de soutènement renforcés a jusqu'à ce jour été restreint aux comparaisons à la pratique du calcul aux contraintes admissibles (ASD) (souvent appelé « calibrage par ajustement »). Cet article porte sur le calibrage LSD pour le cas de l'arrachement du renforcement dans les murs renforcés de géogrilles. Un aspect unique de l'article est une base de données de résistance à l'arrachement comprenant plus de 300 valeurs qui fournissent des données statistiques suffisantes pour permettre le calibrage. Le cadre adopté pour cette étude est basé sur l'approche rapportée par Bathurst et al. (2008). Cinq différents modèles déterministiques d'arrachement, incluant le modèle courant implicite de l'AASHTO/FHWA et le facteur de charge implicite de 1.35 recommandé par l'AASHTO, sont utilisés pour le calibrage. La probabilité de défaillance visée est de 1 dans 100. Pour simplifier les exemples dans l'article, on suppose des valeurs de biais statistique pour les charges. Les modèles déterministiques sont sondés pour des dépendances masquées et un nouveau modèle d'arrachement est proposé. Les résultats de calibrage sont présentés sous forme de tableaux de facteurs de résistance.

1 INTRODUCTION

The American Association of State Highway and Transportation Officials (AASHTO 2007) and the Canadian Highway Bridge Design Code (CSA 2006) are committed to a limit states design (LSD) approach for all transportation-related structures, including reinforced soil retaining walls. LSD requires engineers to use prescribed limit state equations and load and resistance factors specified in design codes. The objective of LSD *calibration* is to compute appropriate load and resistance factor values to give an acceptable probability of exceedance for potential serviceability and failure modes. There are two main challenges for LSD calibration in geotechnical engineering practice: (i) poor prediction accuracy of some underlying deterministic models, and; (ii) lack of data to perform rigorous analysis.

This paper focuses on LSD calibration for the limit state of pullout of geogrid layers in reinforced soil walls. Large databases for both measured reinforcement load in geosynthetic walls and pullout resistance from laboratory tests have been collected by the writers. Due to space limitations, this paper is focussed on the influence of the underlying deterministic pullout model and model bias statistics on the computation of pullout resistance factor. To simplify calculations, load statistics are assumed together with a target probability of pullout failure of 1 in 100 over the design lifetime of the structure, typically 75 years. In addition to quantifying model error, the paper highlights the influence of hidden dependencies between model bias statistics and calculated pullout capacity. Finally, a new pullout model is proposed that improves pullout capacity predictions and removes undesirable hidden dependencies.

2 BACKGROUND

Limit states design (LSD) is a reliability-based design approach, which is fundamentally different from the conventional factor-of-safety (FS) approach. LSD explicitly includes an acceptable estimate of the probability of failure (P_f) for the design limit state under consideration while the FS-based approach does not. The objective of LSD calibration is to estimate the load and resistance factor values such that a prescribed (target) P_f is satisfied. A brief background is necessary to understand the calibration analyses presented later in this paper.

2.1 Limit State Function

The fundamental criterion in LSD is to ensure that, for a specific limit state (g), the resistance (R) must be greater than the load effect (Q). This is expressed by the limit state function

$$g = R - Q \geq 0 \quad [1]$$

The probability of failure ($g < 0$) is related to the overlap area of the frequency distributions for R and Q. In North America, LSD is based on a factored resistance approach that can be expressed as

$$\phi R_n \geq \sum \gamma_i Q_{ni} \quad [2]$$

Here, Q_{ni} = nominal (specified) load; R_n = nominal (characteristic) resistance; γ_i = load factor; and φ = resistance factor. Uncertainty in the calculation of resistance capacity is taken into account by a single resistance factor while (typically) different load factors are applied to multiple load sources. In design codes, the load factor values are always greater than one and the resistance factor values always less than or equal to one. However, for these criteria to apply the underlying deterministic design models must be reasonably accurate.

2.2 Model Bias

Bias (also called model bias) is defined as the ratio of measured to calculated value. Calibrations carried out in this paper are based on bias statistics. This approach has been used by Nowak and co-workers (Nowak 1994, Nowak and Grouni 1994, Nowak and Szerszen 2003, Szerszen and Nowak 2003) for LSD calibration of highway bridge design codes in Canada and the United States. Basic concepts of this approach applied to reinforced soil walls have been described by Bathurst et al. (2008a) and Allen et al. (2005). As the term suggests, model bias values are a quantitative measure of the accuracy of the underlying deterministic load or resistance model used in a limit state function. For a good model, the mean bias value is close to one and the coefficient of variation (COV) is small.

Using the bias concept, Equation 2 can be expressed as

$$X_R \sum \gamma_i \lambda_i \geq \varphi \sum X_{Qi} \lambda_i \quad [3]$$

Here, X_{Qi} = load bias = Q_{mi} / Q_{ni}; X_R = resistance bias = R_m / R_n; Q_{mi} and R_m = measured load and resistance; and λ_i = load ratio (say, Q_{ni} / Q_{n1}). When there is only one load term, such as in the current analysis, Equation 3 reduces to

$$\gamma_Q X_R \geq \varphi X_Q \quad [4]$$

Once the load factors are selected, Equation 3 or 4 can then be used to estimate P_f (LSD design) or the resistance factor value (LSD calibration).

2.3 Probability of Failure and Reliability Index

The first step in LSD calibration is to select a target P_f value. In general, the selection of P_f is related to load capacity redundancy in the structure. Reinforced soil walls are highly redundant systems due to the use of multiple reinforcement layers. Load shedding from one failed reinforcing element to the remaining layers is expected for reinforced soil walls. This is analogous to pile groups for which a P_f value of 1 in 100 was recommended by D'Appolonia (1999) and Paikowsky et al. (2001). The same P_f value was adopted by Bathurst et al. (2008a) and Allen et al. (2005) and is used in the current study.

Civil engineers, especially structural engineers often use reliability index (β index) to specify the P_f magnitude in design. The target P_f value used in the current study of 1 in 100 corresponds to reliability index $\beta = 2.33$.

2.4 Closed-form Solutions and Monte Carlo Method

If the limit state function (Equation 4) is linear and the load and resistance bias values are normally distributed, β can be computed using

$$\beta = \frac{\frac{\gamma_Q}{\varphi}\mu_R - \mu_Q}{\sqrt{\left(\mathrm{COV}_R \frac{\gamma_Q}{\varphi}\mu_R\right)^2 + \left(\mathrm{COV}_Q \mu_Q\right)^2}} \quad [5a]$$

If the bias values are log-normally distributed, then

$$\beta = \frac{\mathrm{Ln}\left[\frac{\gamma_Q}{\varphi}\frac{\mu_R}{\mu_Q}\sqrt{\left(1+\mathrm{COV}_Q^2\right)/\left(1+\mathrm{COV}_R^2\right)}\right]}{\sqrt{\mathrm{Ln}\left[\left(1+\mathrm{COV}_Q^2\right)\left(1+\mathrm{COV}_R^2\right)\right]}} \quad [5b]$$

Here, μ_R and μ_Q are the mean of resistance and load bias values, respectively, and COV_R and COV_Q are the corresponding coefficients of variation. When a closed-form solution does not exist (e.g. normal and log-normal distribution combination) the more adaptable Monte Carlo method can be used to estimate the P_f value. For LSD calibration, the general procedure is to fix the load factor, which is often prescribed, and then assume different resistance factor values until the target P_f or β value is obtained.

3 PULLOUT DATABASE

Rigorous LSD calibration requires statistical information for both the load and resistance data. For this study, they are the maximum reinforcement load in a layer and the corresponding ultimate pullout capacity of the same layer. As noted earlier, this paper is focused on the resistance (pullout capacity) side of the pullout limit state equation.

Reinforcement pullout capacity is generally measured using laboratory pullout tests. Juran et al. (1988) reported a synthesis of experimental pullout data available at that time. Since then the influence of test methodology on the results and interpretation of pullout testing has been

investigated by Farrag et al. (1993) and Palmeira and Milligan (1989), amongst others. However, until recently a large pullout test database from many sources was not available. The writers have compiled a database of more than 500 test results collected from 17 sources. The data sources include published papers, commercial laboratory reports and government certification programs. A total of 318 geogrid pullout data were used to quantify the prediction accuracy of five pullout models. These data were from tests carried out using flexible vertical loading devices such as airbags and pullout boxes meeting the minimum dimensional requirements of ASTM (D6706). The reinforcement types include all three typical commercial geogrid products (uniaxial, biaxial and woven polyester (PET)). The accuracy of five different deterministic models was investigated. No significant statistical differences related to product type were found and hence different pullout models for different product types were not needed. Soils were typical granular materials ranging from sand to gravel. Confining pressures in the laboratory tests ranged up to 120 kPa and measured pullout loads were less than 80 kN/m.

4 CALIBRATION

As mentioned earlier, the target P_f is set at 1 in 100. Clearly there are an infinite number of combinations of load and resistance factor values that can satisfy a prescribed P_f value. In this analysis, a load factor γ_Q = 1.35 recommended by AASHTO (2007) is used and the corresponding resistance factor computed.

4.1 Bias Statistics for Geogrid Pullout Resistance

According to AASHTO (2007) and FHWA (2001) the pullout capacity (P_c) for sheet geosynthetics (geotextiles and geogrids) is estimated using

$$P_c = 2F^* \alpha \sigma_v L_e \qquad [6]$$

Here, σ_v = normal stress at elevation of the reinforcement layer, L_e = anchorage length, F^* and α = dimensionless parameters. In the FHWA document, the following default values are recommended: α = 0.8 for geogrids and α = 0.6 for geotextiles, and F^* is related to the peak soil friction angle (ϕ_s) by

$$F^* = \frac{2}{3}\tan\phi_s \qquad [7]$$

Equation 6 shows that for a specific combination of soil and reinforcement specimen, predicted pullout resistance is linearly proportional to vertical stress. This contradicts some pullout test data presented later where the measured pullout capacity is shown to be much greater than the predicted value under low confining pressures. This phenomenon is related to the dilation of soil in the vicinity of the reinforcement-soil interface (Juran et al. 1988).

In this paper five deterministic pullout models with different prediction accuracy, including the current default AASHTO/FHWA pullout model, are investigated.

4.1.1 Model 1: using average measured F*α value

Model 1 is based on back-calculation of a single value for F*α using the average of multiple tests carried out on the same soil with a single geogrid product and reinforcement length under different normal stress (one test series). This model is typically used to interpret the results of product-specific laboratory testing with one soil material.

Figure 1a shows the measured versus calculated pullout resistance values using Model 1. The data fall evenly about the 1:1 correspondence line with little spread. The bias mean and COV are 1.00 and 0.21, respectively (Table 1). However, the bias values tend to decrease with increasing calculated resistance values (Figure 1b). A zero-slope test (Draper and Smith 1981) performed on this data reveals that the 95% confidence interval on the slope of the linear regression line does not include the zero value. This is quantitative evidence that there is significant relationship (dependency) between the parameters in this plot (at a level of significance of α = 5%) and hence using Equations 5a and 5b with statistics for the entire data set is not valid (i.e. there is hidden error). One strategy to remove this undesirable dependency is to parse the data into different groups and divide each data point in a group by the average group

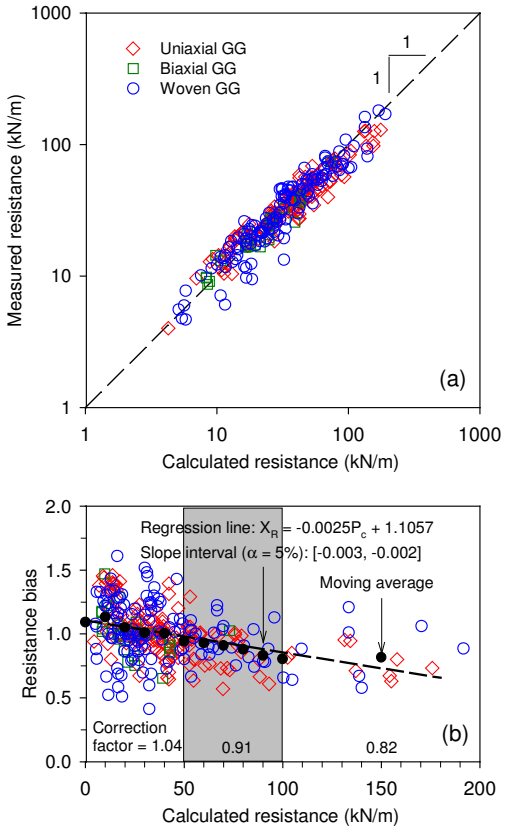

Figure 1.[0] Prediction accuracy using Model 1: (a) Measured versus calculated pullout resistance values;[0] (b) Dependency between resistance bias and calculated values.

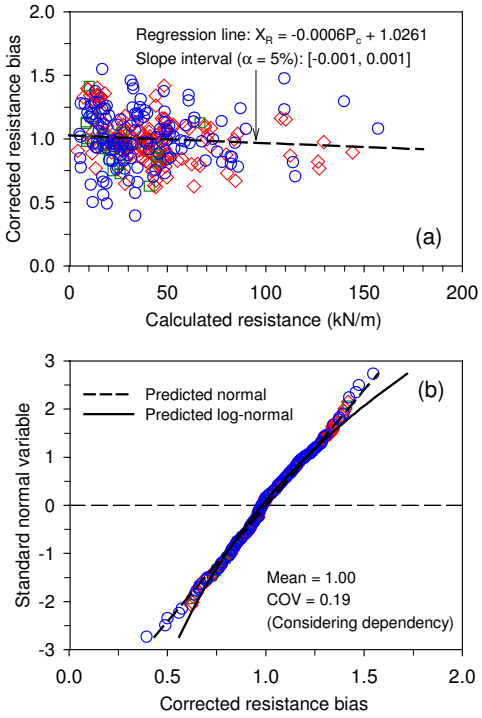

Figure 2. Resistance bias statistics for Model 1 after removing dependency: (a) Corrected resistance bias values versus calculated resistance; (b) CDF plots of corrected resistance bias values.

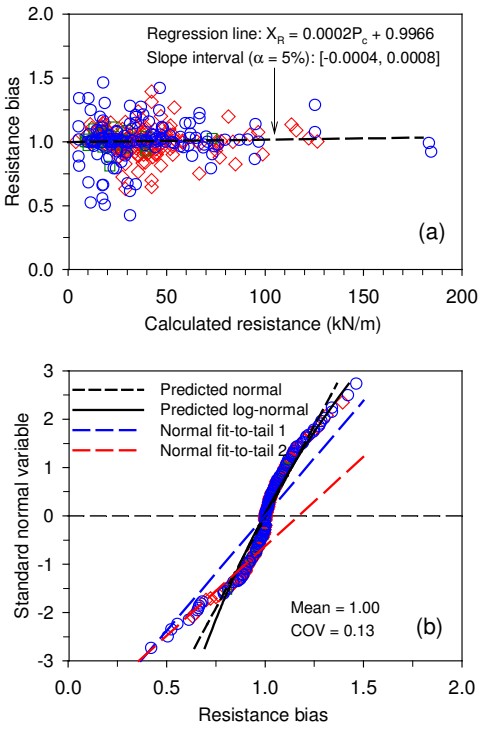

Figure 3. Resistance bias statistics for Model 2: (a) Bias versus calculated resistance values; (b) CDF plots of bias values.

value (correction factor). The moving average values (solid symbols in Figure 1b) suggest convenient break points at 50 and 100 kN/m. The correction factor values are given in the figure.

The zero-slope test applied to the corrected data shows that the earlier dependency has been removed (Figure 2a). A cumulative distribution function (CDF) plot is presented in Figure 2b for the corrected resistance bias values together with approximations to the data using normal and log-normal distributions.

4.1.2 Model 2: using 1st-order approximation to measured $F^*\alpha$ values

An alternative approach to Model 1 is to fit a first-order polynomial approximation to $F^*\alpha$ versus normal stress data. This is expected to better capture stress-level dependency of pullout capacity. Since $F^*\alpha$ values generally decrease with increasing normal stress, the linear regression should show a negative slope. Model 2 reduces to Model 1 if the range of normal stress is narrow and (or) the magnitude of normal stress is very high.

Figure 3a plots bias values against calculated pullout resistance using Model 2. As expected, there is no visual dependency. Also, zero slope of the regression line is included in the 95% confidence interval [-0.0004, 0.0008]. The bias mean remains one but the COV value of 0.13 is lower than COV = 0.19 using Model 1.

Figure 3b shows the CDF plot and the normal and log-normal approximations to the bias data. For the resistance data in LSD calibration, it is the lower tail of the distribution that makes a major contribution to the computed P_f value. Here, neither the normal or log-normal distribution using all the data can fit the lower tail satisfactorily. Since the selection of best fit-to-tail distribution is subjective, two fit-to-tail CDF curves are given in Figure 3b. The resistance factor values using the best fit-to-tail distributions are reported later in the paper.

4.1.3 Model 3: AASHTO (FHWA) approach with default coefficients

The underlying deterministic model with default coefficients is described in Section 4.1. Figure 4a shows the measured versus predicted pullout resistance using Model 3. Most (about 90%) of the data fall above the 1:1 correspondence line. The computed bias mean is about 2.21. Hence, Model 3 underestimates the pullout capacity by a factor greater than two *on average*. However, this bias mean value is misleading if the hidden dependency is not considered. Figure 4b shows that there is pronounced dependency between the bias and calculated resistance values. In fact, when the calculated resistance values are greater than 30 kN/m, almost all data are less than the mean bias value.

One way to quantify the influence of the hidden dependency is to fit a power function curve to the bias versus calculated resistance data (Figure 4b). This power function is used later to propose an improved pullout model (Model 5). It is noted that there is a fundamental

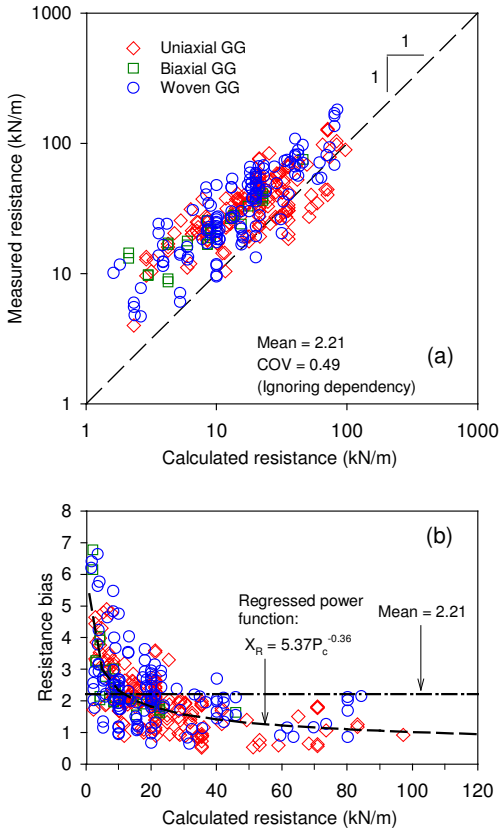

Figure 4.[0] Prediction accuracy using Model 3: (a) Measured versus calculated pullout resistance values; (b) Dependency between resistance bias and calculated values.

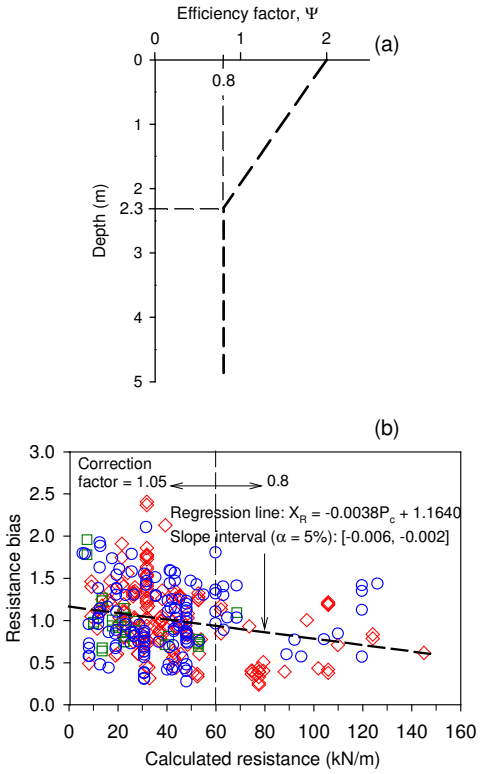

Figure 5. Model 4 prediction accuracy: (a) Efficiency factor versus depth assuming γ = 17.5 kN/m^3. (b) Dependency between resistance bias and calculated values.

difference between Model 3 and Model 5. Model 3 assumes a linear relationship between pullout capacity and normal stress while Model 5 assumes a nonlinear relationship. The latter is consistent with observations made by some researchers from results of laboratory pullout tests. Similar to adjustments made to Model 1, this power function can also be used to compute correction factors to remove bias dependency. The quantitative influence of ignoring and correcting for hidden bias dependency on factored resistance values is discussed later in the paper.

4.1.4 Model 4: Bi-linear pullout model

The nonlinear relationship between pullout capacity and normal stress can be approximated using a bi-linear distribution of the efficiency factor (ψ) with normal stress. Here ψ is defined as $F^*\alpha$ divided by tan ϕ_s. Current design codes also use bi-linear functions to estimate the coefficient of earth pressure used in the calculation of reinforcement loads for steel reinforced soil walls (e.g. AASHTO 2007). Using the optimization solver in Microsoft Excel, the writers propose the bi-linear efficiency factor distribution (Model 4 here) shown in Figure 5a.

Using Model 4, the bias mean is close to one and the COV is about 0.40 (Table 1). Compared to Figure 4b, the visual impression from Figure 5b is that the dependency between bias values and calculated resistance is much less but nevertheless detectable as shown by the linear regression line superimposed on the data. This is confirmed by the calculation of the 95% confidence interval on the regression line slope which does not contain the zero slope value. In order to analyze the influence of the hidden dependency, the same technique used earlier for Model 1 was used on the bias data here. As shown in the figure, the correction factor values are 1.05 and 0.8 above and below the selected break point of 60 kN/m, respectively. For brevity, plots similar to Figure 2 are not shown for corrected Model 4 bias data.

4.1.5 Model 5: Non-linear pullout model

A shortcoming of Model 4 is that there are remaining hidden dependencies from sources other than vertical stress. In order to remove all bias dependency, Model 5 uses the power function fitted to the data in Figure 4b to adjust the current AASHTO/FHWA default pullout model (Model 3). Implementation of Model 5 is a two-step process. First, calculate the pullout capacity using Equation 6 with default coefficients; then, correct this value using the power function expression presented in Figure 4b. It should be noted that the power function coefficients are dimension-dependent (here, in units of kN/m). The two-step process can be expressed as

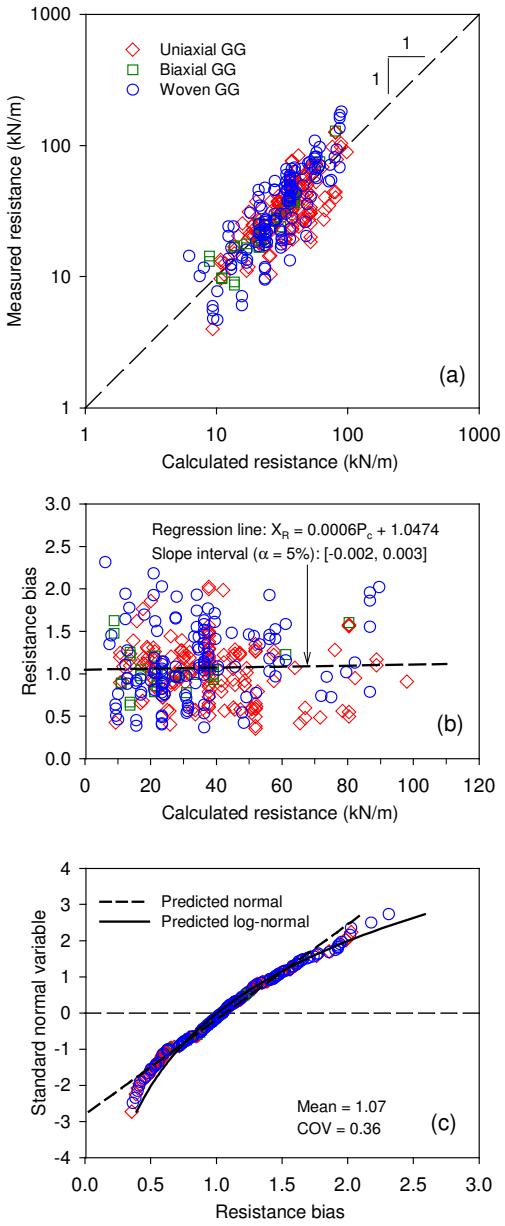

Figure 6. Prediction accuracy using Model 5: (a) Measured versus calculated pullout resistance values; (b) Dependency between resistance bias and calculated values; (c) CDF plots of resistance bias values.

$$P_c(\text{corrected}) = 5.37P_c^{0.64}(\text{kN/m}) \quad [8]$$

Figure 6 illustrates the prediction accuracy of Model 5. All measured versus predicted pullout load data fall close to the 1:1 correspondence line. The bias mean is about 1.07 and the COV is less than 0.4. Moreover, the zero-slope test indicates that the dependency between the bias and calculated resistance values is negligible. These are marked improvements over Model 3 that is currently used in most design codes. Figure 6c indicates that the log-normal approximation to the data on a CDF plot provides a better approximation than a normal distribution.

4.2 Bias Statistics for Load

Issues related to load model accuracy and potential hidden error in load models are equally important in LSD calibration as accuracy and hidden dependencies in resistance models. The current approach for the calculation of reinforcement load in geosynthetic reinforced soil walls is the AASHTO (2007) Simplified Method. This method has been demonstrated to be excessively conservative (Allen et al. 2002, 2003; Bathurst et al. 2008b). To overcome this problem Allen, Bathurst and co-workers have proposed a new empirical method, called the K-Stiffness Method, to estimate reinforcement loads under operational conditions. Including load bias statistics in the calculations to follow using the AASHTO Simplified Method or the K-Stiffness Method cannot be done in the space provided. However, to illustrate the general approach, load bias values are assumed to be log-normally distributed with a mean value equal to one and COV varying from 0.1 to 0.5.

4.3 Example Calibration Results

Table 1 summarizes bias statistics for the five pullout resistance models. It is assumed that the bias values are normally distributed for the first two models and log-normally distributed for the last three models. Bias statistics that ignore dependency (e.g. Figure 1b) and bias statistics that are corrected to remove dependency (e.g. Figure 2a) are only slightly different for Models 1 and 4.

Table 2 shows the computed resistance factor φ values for $\beta = 2.33$ and $\gamma_Q = 1.35$. As may be expected, for all resistance models the computed φ value decreases as the COV of load bias increases. Except for Model 3, the bias mean of all other models are close to one and hence are easy to compare. In general, Models 1 and 2 yield φ values closer to one than Models 4 and 5. This can also be expected since the first two resistance models are typically based on product- and soil-specific testing and hence the scatter in bias data (COV) is smaller; while the last two general models produce larger data scatter. Calibration results for Models 1 and 4 show that, if hidden dependency is not taken into account, the computed φ value could result in significant over- or under-design depending on the calculated resistance value. Table 3 shows φ values computed using best fit-to-tail distributions for Model 2. Comparison with fitting to the entire bias value data shows that best fit-to tail results in lower resistance values. The latter approach is judged to be better since it captures the distribution at the lower tail which strongly influences the probability of failure.

Finally, the influence of hidden dependency in Model 3 is presented in Figure 7. The ratio of factored resistance value considering dependency ($R_{cd} = \varphi P_c(\text{corrected})$) to the same value but ignoring dependency ($R_{id} = \varphi P_c$) varies from greater than one for calculated pullout values less than 30 kN/m to less than one for calculated pullout capacity values greater than 30 kN/m. A practical implication of the curve in Figure 7 is

that ignoring dependency results in non-conservative (unsafe) design (P_f > 1/100) if the calculated resistance is greater than 30 kN/m and results in conservative (safe) design (P_f < 1/100) if the calculated resistance is less than 30 kN/m.

5 CONCLUSIONS

This paper presents the influence of model prediction accuracy on calculation of resistance factor in LSD calibration using five different geogrid pullout models and a large pullout database compiled by the writers. An attempt has been made to quantify the calibration error due to hidden dependency between the bias and predicted values. This has highlighted the importance of considering not only model bias in LSD calibration but also the quantitative effects of considering and ignoring hidden dependencies. In addition, special attention to the tails of CDF plots of basic random variables is always required even though the selection of best fit-to-tail distribution is subjective.

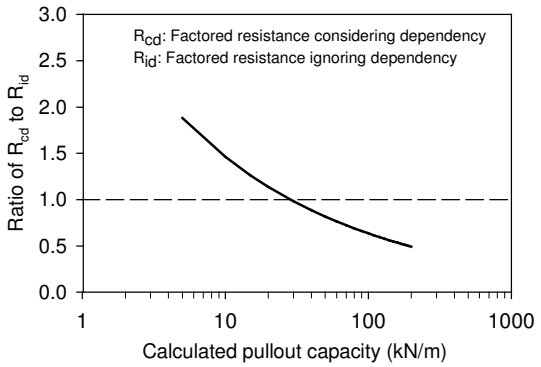

Figure 7.[0] Influence of hidden dependency on computed factored resistance capacity using Model 3.

ACKNOWLEDGEMENTS

The research reported here was funded in part by the Natural Sciences and Engineering Research Council of Canada, the Ministry of Transportation of Ontario and a consortium of 12 USA departments of transportation.

REFERENCES

AASHTO. 2007. LRFD bridge design specifications. 4th ed., AASHTO, Washington, DC, USA.

ASTM D 6706-01. 2001. Standard test method for measuring geosynthetic pullout resistance in soil, ASTM, West Conshohocken, PA, USA.

Allen, T.M., Bathurst, R.J. and Berg, R.R. 2000. Global level of safety and performance of geosynthetic walls: An historical perspective. *Geosynthetics International*, 9(5-6): 395–450.

Allen, T.M., Bathurst, R.J., Holtz, R.D., Walters, D.L. and Lee, W.F. 2003. A new working stress method for prediction of reinforcement loads in geosynthetic walls. *Canadian Geotechnical Journal*, 40: 976-994.

Allen, T.M., Nowak, A.S. and Bathurst, R.J. 2005. Calibration to determine load and resistance factors for geotechnical and structural design. *Transportation Research Board Circular E-C079*, Washington, DC, 93 p.

Bathurst, R.J., Allen, T.M. and Nowak, A.S. 2008a. Calibration concepts for load and resistance factor design (LRFD) of reinforced soil walls. *Canadian Geotechnical Journal*, 45: 1377-1392.

Bathurst, R.J., Miyata, Y., Nernheim, A. and Allen, T.M. 2008b. Refinement of K-Stiffness Method for geosynthetic reinforced soil walls. *Geosynthetics International*, 15(4): 269-295.

CSA. 2006. Canadian highway bridge design code (CHBDC). Canadian Standards Association (CSA), Toronto, ON, Canada.

Draper, N.R. and Smith, H. 1981. *Applied regression analysis*, 2nd ed., John Wiley & Sons, New York, NY, USA.

Farrag, K., Acar, Y.B. and Juran, I. 1993. Pullout resistance of geogrid reinforcements. *Geotextiles and Geomembranes*, 12: 133-159.

Federal Highway Administration. 2001. Mechanically stabilized earth walls and reinforced soil slopes — design and construction guidelines. FHWA-NHI-00-043, (editors Elias, Christopher, & Berg), Federal Highway Administration, Washington, DC, USA.

Juran, I., Knochenmus, G., Acar, Y.B. and Arman, A. 1988. Pullout response of geotextiles and geogrids (Synthesis of available experimental data), Geosynthetics for soil improvement, Holtz, R.D., Editor, Geotechnical Special Publication No.18, ASCE, Proceedings of a symposium held in Nashville, Tennessee, USA, May 1988, pp. 92-111.

Nowak, A.S. 1994. Load model for bridge design code. *Canadian Journal of Civil Engineering*, 21: 36-49.

Nowak, A.S. and Grouni, H.N. 1994. Calibration of OHBDC-1991. *Canadian Journal of Civil Engineering*, 21: 25-35.

Nowak, A.S. and Szerszen, M.M. 2003. Calibration of design code for buildings (ACI 318): Part 1-Statistical models for resistance, *ACI Structural Journal*, 100(3): 377-382.

Paikowsky, S.G. 2004. Load and resistance factor design (LRFD) for deep foundations. NCHRP Report 507, National Cooperative Highway Research Program, Transportation Research Board, Washington, DC, USA.

Palmeira, E.M. and Milligan, G.W.E. 1989. Scale and other factors affecting the results of pullout tests of grids buried in sand, *Geotechnique*, 39(3): 511-524.

Szerszen, M.M. and Nowak, A.S. 2003. Calibration of design code for buildings (ACI 318): Part 2-Reliability analysis and resistance factors, *ACI Structural Journal*, 100(3): 383-391.

Table 1. Summary of resistance bias statistics.

Resistance prediction method	Distribution type	Maximum	Minimum	Mean (μ_R)	COV_R	Dependency
Model 1	Normal	1.61	0.41	1.00	0.21	Ignored
	Normal	1.55	0.39	1.00	0.19	Considered
Model 2	Normal	1.46	0.42	1.00	0.13	None
Model 3	Log-normal	6.77	0.52	2.21	0.49	Ignored
Model 4	Log-normal	2.41	0.24	1.01	0.40	Ignored
	Log-normal	2.29	0.26	1.00	0.39	Considered
Model 5	Log-normal	2.31	0.35	1.07	0.36	None

Table 2. Computed resistance factor φ for $\beta = 2.33$ and $\gamma_Q = 1.35$.

Resistance prediction method	Assumed load bias statistics ($\mu_Q = 1$)					Dependency
	$COV_Q = 0.1$	$COV_Q = 0.2$	$COV_Q = 0.3$	$COV_Q = 0.4$	$COV_Q = 0.5$	
Model 1	0.78	0.71	0.61	0.53	0.48	$P_c \leq 50$ kN/m
	0.68	0.62	0.54	0.46	0.42	$50 \leq P_c \leq 100$ kN/m
	0.62	0.56	0.48	0.42	0.38	$P_c > 100$ kN/m
	0.68	0.61	0.56	0.50	0.44	Ignored
Model 2	0.89	0.78	0.66	0.56	0.48	None
Model 3	0.89	0.84	0.78	0.71	0.64	Ignored
Model 4	0.54	0.50	0.45	0.41	0.36	$P_c \leq 60$ kN/m
	0.41	0.38	0.35	0.31	0.28	$P_c > 60$ kN/m
	0.50	0.47	0.43	0.38	0.34	Ignored
Model 5	0.59	0.54	0.49	0.44	0.39	None

Note: P_c = calculated pullout value using deterministic model

Table 3. Computed resistance factor φ using best fit-to-tail distributions for Model 2 ($\beta = 2.33$, $\gamma_Q = 1.35$).

Fit-to-tail curve (Figure 4b)	Assumed load bias statistics ($\mu_Q = 1$)				
	$COV_Q = 0.1$	$COV_Q = 0.2$	$COV_Q = 0.3$	$COV_Q = 0.4$	$COV_Q = 0.5$
Curve 1 ($\mu_R = 1$, $COV_R = 0.21$)	0.68	0.61	0.56	0.50	0.44
Curve 2 ($\mu_R = 1.17$, $COV_R = 0.27$)	0.75	0.68	0.59	0.51	0.46